Dalton Transactions

Accepted Manuscript

ROYAL SOCIETY OF CHEMISTRY

www.rsc.org/dalton

Investigation on Spin-Flip Reaction of Re + CH_3CN by Relativistic Density Functional Theory

Yi Xiao, Wen-Xin Ji, Wei-Xu, Xian-Yang Chen, and Shu-Guang Wang*

School of Chemistry and Chemical Engineering, Shanghai Jiao Tong University, 200240 Shanghai, China

Abstract: To explore the integrated reaction mechanisms for Re atom with acetonitrile theoretically, density functional theory with zero-order regular approximation (ZORA) relativistic corrections has been employed at the BP86/TZ2P level. There have been three adiabatic potential energy surfaces in the study along sextet, quartet and doublet spin states. However, the detailed minimum energy reaction pathway altogether contains six stationary states (**1**) to (**6**), five transition states (**TS**), and two intersystem crossings with spin inversion (marked by ⇒): ^{6}Re + CH_3CN → η^1-$ReNCCH_3$ (^{6}**1**) → ^{6}**TS$_{1/2}$** ⇒ η^2-$Re(NC)CH_3$ (^{4}**2**) → ^{4}**TS$_{2/3}$** → η^3-$HRe(NCCH_2)$ (^{4}**3**) → ^{4}**TS$_{3/4}$** → CH_3-ReNC (^{4}**4**) → ^{4}**TS$_{4/5}$** → CH_2=Re(H)NC (^{4}**5**) ⇒ ^{2}**TS$_{5/6}$** → CH≡$Re(H)_2NC$ (^{2}**6**). Thereinto, the lowest energy crossing points (LECP) have been determined by the DFT fractional-occupation-number (FON) approach. The first spin inversion has transferred the PESs from high-spin sextet to the quartet intermediate (^{4}**2**) with the subsequent C-C bond breakage. The second one from the quartet to the low-spin doublet state accompanies with the C-H activation, decreasing the transition barrier by 157 kJ/mol. The overall reaction could be exothermic by about 210 kJ/mol. Harmonic vibration frequencies and NBO, WBO analysis are also applied to verified the experimental observed information.

Keywords: rhenium; acetonitrile; reaction mechanism; potential surface bounding; spin transitions; minimal energy crossing points; density functional approach; fractional occupation number approach.

---

* To whom correspondence should be directed, Email: sgwang@sjtu.edu,cn

1. Introduction

Owing to the developed technologic measures, the violation of "spin-forbidden" reactions of transition metals (TM) in gas-phase[1-3] have been detected which verified experimentally the probability for two-state reactivity (TSR)[4-6] or multiple-state reactivity (MSR)[7-10] mechanisms. The researches concerning the activation of C-H(X) and C-C bond in small alkanes and halomethanes with TMs[11-17] are always the subject of scientists' attention in decades due to the potential environmental and economic significance. The investments in both experimental and theoretical aspects have expressly harvested the organometallic species and the overall mechanism of TM catalyst.[18-24] Recently the reactions of nitriles with a series of TMs[25-28] result from the interaction of electron-rich species with relative electron-deficient TMs also revealed the activations and identified the series of sophisticated products.

The intersystem crossings are often deemed to exist in these type reactions involving several different spin symmetric potential energy surfaces (PES). In the TSR or MSR, spin crossings are the fundamental mechanism for accelerating[29] the reaction under different spin-symmetric states. At the nonrelativistic approximation level, surface crossing for the N-atom system actually forms one 3N-7 dimensional crossing seam along two adiabatic PESs with different spin multiplicities. Then the Low Energy Crossing Region (LECR) of two different spin PESs could be easily reached by guiding reaction wave-packet crossover through thermal activation. One 3N-8 dimensional transition structure i.e. Minimum Energy Crossing Point (MECP) should exist in the LECR. To explore such reactions is still a challenge for the theoretical chemists. There are two difficulties should be solved, one is the complexity of two-electron correlation and one-electron relativistic (including mass-velocity, Darwin and Spin-Orbit Coupling (SOC)[30-31]) effects in the open d-shell TM atoms. Second is how to determine the transition structure on the Minimum Energy Crossing Point (MECP).

Under the Born-Oppenheimer approximation, nonadiabatic coupling (SOC) makes it possible for spin inversion in which the MECP lies energetically somewhat below the LECR. There are some conditions: 1). For the identically spin-inversion transition structure, the energies under two electron-spin states should be the same i.e. Frank-Condon principle should be fulfilled; 2) the transition position would lies the lowest potential on the crossing seam. Some methods have been applied to solve the difficulty for the orientation of MECP. Multiple-Configuration Wave function

(e.g. MCSCF or CASSCF) and Density Functional Theory (DFT) based procedures[32-38] are often worked. One general process is first achieving the energies and gradients for series of structures in two spin PESs along reaction pathway. Then, to use an interfaced subroutine treats these results for drawing near the crossing point gradually. Here, we apply the Fractional Orbital Occupation Number (FON)-DFT approach[39] suggested by us for the type of reactions[39-42].

Besides the C-H and C-C bonds activation for small alkanes, recently the reactions for nitriles with TMs have found many novel insights by Andrews and his cooperators. From the group IV–VI metals with acetonitrile[25-27], methylidyne products have been rarely observed, however, the latter group Re atom reacting with acetonitrile finally generates the methylidyne complex which is observed in 2012 by Cho and Andrews[28]. They had assigned experimentally the possible products by using infrared spectroscopy in the argon matrix, some theoretical calculations had also been done to confirm the structures of intermediates. None of the intersystem crossing information was reported although the reactant and product are with different spin multiplicities. There is still much space for theoretical discussion to the complicated reaction mechanisms in such kind reactions. In this work, we will investigate the reaction chain as follows in detail:

$$\mathrm{Re} + \mathrm{CH_3CN} \rightarrow \eta^1\text{-}\mathrm{ReNCCH_3}\ (\mathbf{1}) \rightarrow \eta^2\text{-}\mathrm{Re(NC)CH_3}\ (\mathbf{2}) \rightarrow \eta^3\text{-}\mathrm{HRe(NCCH_2)}\ (\mathbf{3})$$

$$\rightarrow \mathrm{CH_3\text{-}ReNC}\ (\mathbf{4}) \rightarrow \mathrm{CH_2{=}Re(H)NC}\ (\mathbf{5}) \rightarrow \mathrm{CH{\equiv}Re(H)_2NC}\ (\mathbf{6}) \qquad (1)$$

Here the energies and structures of all various intermediates and transition points will be given with the sextet, quartet and doublet spin states. Then, the spin inversion process will be explored for the MECPs by the FON-DFT approach. Meanwhile, harmonic frequency and NBO analysis also contribute to all equilibrium species.

2. Computing Method

The quantum chemistry calculation has been adopted to explore the feasible reaction mechanism and spin-crossing process of transitional metal Re with CH_3CN. Most calculations were achieved based on density functional theory (DFT), the Amsterdam ADF2012 program, commenced by Baerends.[43-45]

The inner shell electrons considered as the core shells due to low probability of getting activity in molecules were calculated by the fully relativistic Dirac-Slater method,[46] and then transferred

unchanged into the molecules. On this model, the frozen-core approximation was adopted for the atoms C($1s^2$), N($1s^2$) and Re($1s^2$-$4d^{10}$). The valence electrons of all atoms were described by the standard triple-ζ Slater-Type-Orbital (STO) basis sets with two sets of polarization functions (TZ2P).[47] The density functional was applied by the Vosko-Wilk-Nusair (VWN)[48] correlated local-spin-density potential and the density gradient corrections for exchange correlation of the Becke-Perdew (BP).[49-50] Several other generalized gradient approximations such as Perdew-Wang (PW91)[51] and Perdew-Burke-Ernzerhof (PBE)[52] for exchange correlation corrections were also tested. The relativistic scalar Zero Order Regular Approximation (ZORA)[53] was adopted to correct the relativistic effects due to the heavy transition metal Re.

To demonstrate the rationality of reaction pathway, the Intrinsic Reaction Coordinate (IRC)[54-55] procedure was used to follow the minimum energy path in both forward and backward directions from each transition state. All equilibrium and transition state structures were fully optimized. In addition, all analytic harmonic frequencies were also achieved for the characterization of each structure and the corresponding vibrational zero point energy (ZPE) could be included. All the calculations were built on the same theoretical level.

Wiberg Bond Order (WBO)[56] and Weinhold Bond Orbital (NBO)[57] analyses were performed for products at the BP86-DFT level with the help of Gaussian09[58] program, applying the SDD[59] (including a relativistic effective core potential for Re) and 6-311++G(3df, 3pd) basis sets[60] for the metal and the lighter atoms, respectively.

3. Results and Discussion

Relative to the ground state, two lowest excited state energies of Re atom are shown in Table 1. Table 2 lists the ZPE-corrected energies (relative to Re (^{6}S) + CH_3CN) for each equilibrium and transition state in the sextet, quartet and doublet spin states along reaction pathways, respectively. Table 3 presents the theoretical and experimental vibrational frequencies of intermediates for confirmation. Table 4 gives the vibrational frequencies, NBO charges, WBO bond orders and spin density, etc. of the major products CH_2=Re(H)NC and CH≡$Re(H)_2$NC in the three spin states. Three spin-restricted PESs (labeled in different color) and two probable project crossing points (PCPn) are pictured in Fig. 1. Fig. 2 provides the optimized parameters of all stationary and transition structures

among processes.

3.1 Energy Splitting between Electronic States of Re Atom.

From experimental atomic spectroscopy data[61] with relative weighted average of spin-orbit coupled levels, the ground state of Re is sextet ^{6}S ($5d^5 6s^2$). The first and second excited state are sextet ^{6}D ($5d^6 6s^1$) and quartet ^{4}G ($5d^5 6s^2$) which need excited energies of 101 and 126 kJ/mol from the ground sextet ^{6}S state of Re, respectively. Here, we have applied the Baerends method[62] to calculate the atomic excitation energies, avoiding the present DFT deficiency in atomic degenerate densities respect. Three BPE/PW91/BP86 DFT methods are adopted both on relativistic and non-relativistic levels to compare with the experimental values.

Table 1. Energy (in kJ/mol) Differences[a] between Ground and Excited Electronic States of Re.

State	^{6}S	^{6}D	^{4}G
Slater determinant[b]	$(6s)^{\alpha\beta}(5d_0)^{\alpha}(5d_{\pm1})^{2\alpha}(5d_{\pm2})^{2\alpha}$	$(6s)^{\alpha}(5d_0)^{\alpha\beta}(5d_{\pm1})^{2\alpha}(5d_{\pm2})^{2\alpha}$	$(6s)^{\alpha\beta}(5d_0)^{\beta}(5d_{\pm1})^{2\alpha}(5d_{\pm2})^{2\alpha}$
PBE	0	42.4 (Δ58.4)[d]	97.5 (Δ28.0)
PW91	0	44.8 (Δ56.0)	102.3(Δ23.2)
BP86	0	42.0 (Δ58.8)	102.1(Δ23.4)
ZORA+PBE	0	126.3(Δ25.5)	131.0(Δ5.5)
ZORA+PW91	0	122.8(Δ22.0)	130.2(Δ4.7)
ZORA+BP86	0	122.2(Δ21.4)	130.4(Δ4.9)
Exp[c]	0	100.8	125.5

[a] Relative energies versus Re (^{6}S). [b] In $D_{\infty h}$ symmetry. [c] From spectroscopy[61].

[d] Deviation from the experimental values.

The orbital occupations and corresponding energies between ground and excited states are shown in Table 1. There is d_0–d_0 transition ($\alpha \rightarrow \beta$) from ^{6}S to ^{4}G, on the non-relativistic level, the exited energy differences from the experimental values are 28, 23, 23 kJ/mol at the BPE, PW91, and BP86 DFT levels, respectively. With the relativistic corrections, the deviations from experimental value become to only 6, 5, 5 kJ/mol at the BPE, PW91, and BP86 DFT levels, respectively. The relativistic corrections reduce the calculated errors distinctly. However, seen in Table 1, BPE/PW91/BP86 DFT could not give the proper prediction for the first excitation to ^{6}D. At the

non-relativistic level, the calculated excitation energies of ^{6}D state are underestimated by 56~59 kJ/mol compared to experimental data. Relativistic effects make the 6s orbital stable and 5d orbital unstable. After relativistic corrections, the DFT excitation energies of ^{6}D become overestimated by 26, 22, 21 kJ/mol from the BPE, PW91, and BP86 DFT levels, respectively. As known, relativistic effects make the s orbital contractive, causing the d orbital radial distribution expansive, the electron transition between ^{6}S and ^{4}G is only d_0 turned from α to β, while from ^{6}S to ^{6}D is s-d electron promotions. So, relativistic changing is more in ^{6}D term than in ^{4}G term.

From the atomic calculations, we think DFT with ZORA relativistic correction is suitable to reproduce the various electronic states of Re contained molecules. In this work, we choose the ZORA-BP86 method with the TZ2P-STO basis set to investigate the reaction mechanisms of Re + CH_3CN system.

3.2 The Spin-Sextet Reaction Mechanism for Re (^{6}S) + CH_3CN system

Table 2. ZPE-Corrected Energies[a] (in kJ/mol) of Each Stationary and Transition State Relative to Re (^{6}S) + CH_3CN among the Spin-Doublet, -Quartet and -Sextet Reactions.

Species	Sextet	Quartet	Doublet
Re:	$d^5s^2\ ^6S$	$d^5s^2\ ^4G$	$d^5s^2\ ^2D$
Re+CH_3CN	- 0 -	+130.4	+257.8
1	-13.6(~0.3)[b]	-38.2(~23)	14.5
$TS_{1/2}$	-11.05	31.3	98.8
2	-43.1(~24)	-76.7(~15)	-70.3(~35)
$TS_{2/3}$	60.0	59.1	82.0
3	-54.6	-99.3	-78.8
$TS_{3/4}$	115.4	97.0	130.8
4	-102.9(~-58)	-104.0(~-40)	-42.6(~17)
$TS_{4/5}$	51.4	-88.9	-36.9
5	20.4	-144.0(~-62)	-142.2(~-45)
$TS_{5/6}$	184.1	11.4	-145.7
6	162.4	6.3	-210.3(~-102)

a) ZPE-Corrected, from spin-orbit averaged (SOA) ZORA-BP86-TZ2P/STO DFT.

b) The energy with the incorrect structure **1** at B3LYP level by Cho and Andrews in their Table, according to their procedure. All bracket values at 6-311++G(3df, 3pd)/ B3LYP level[28].

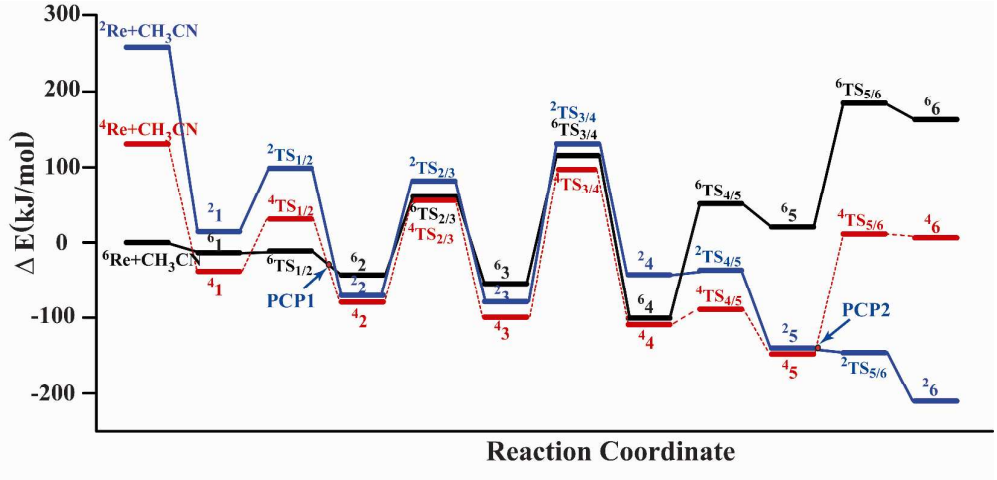

Fig. 1 The PES curves with the spin-unrestricted option along the reaction pathway Re + CH_3CN → $CH{\equiv}Re(H)_2NC$. (In kJ/mol)

The ground state of Re atom is $5d^5 6s^2$ (^{6}**S**). The d-shell should be filled in half-charged state in according with the Hund rule. However, the ground state of product $CH{\equiv}Re(H)_2NC$ (**6**) is in a doublet state experimentally observed[28]. Intersystem crossing must occur somewhere. Here, the spin-restricted reaction mechanism for the sextet Re atom with CH_3CN is studied. Starting from Re atom with ground state (^{6}**S**) attaching to acetonitrile, the first step forms straightway the complex Re···$NCCH_3$ (^{6}**1**). The dative bond length is 2.17 Å and the stabilization energy is about 14 kJ/mol, lower than that of the reactants, as shown in Fig.1 and Fig.2. However, the second step could easily occur due to one negligible energy barrier of the transition state ^{6}**TS$_{1/2}$**, the nitrile π complex (η^2-Re(NC)CH_3) (^{6}**2**) is generated and releasing energy about 30 kJ/mol. The Re moves to above the nitrile which draws Re and C1 as near as 2.11 Å.

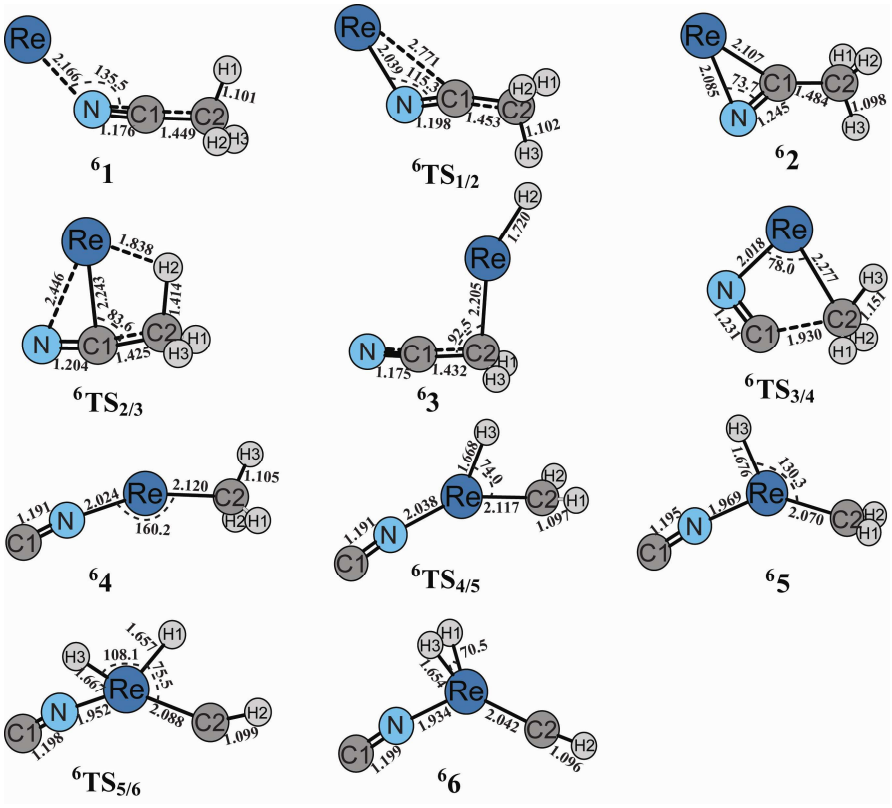

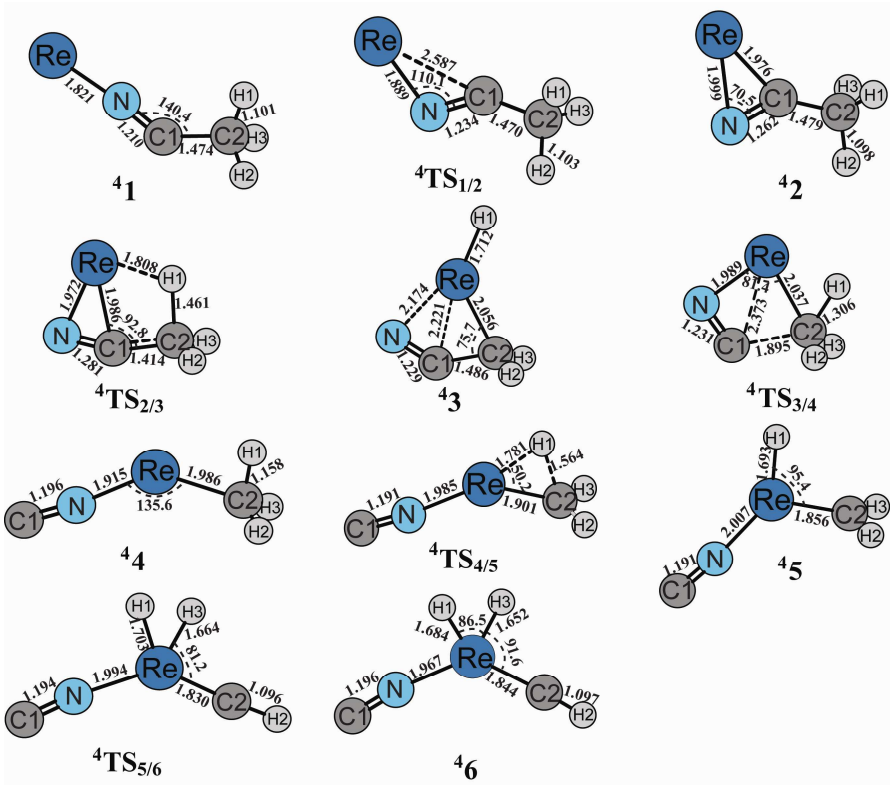

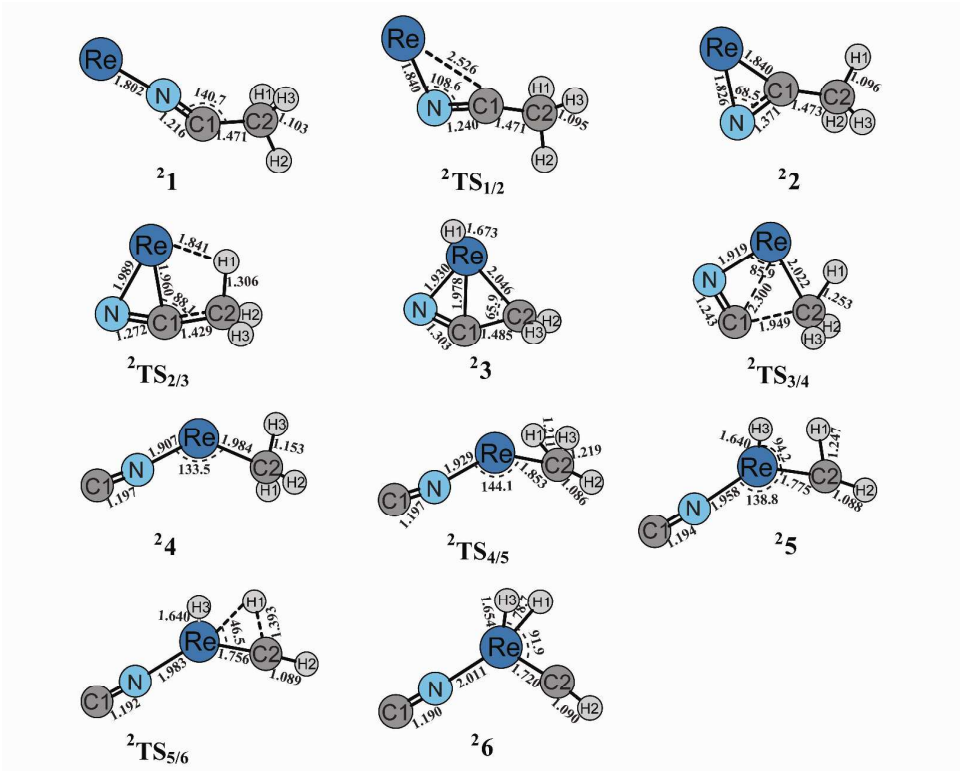

Fig. 2 Optimized equilibrium geometric structures of the important intermediates in the reaction of Re + CH_3CN with sextet, quartet, and doublet spin states (distances in Å, angles in ^{o}).

Then, the η^2-Re(NC)CH_3 (^{6}**2**) would convert over an obvious transition barrier of ^{6}**TS$_{2/3}$** forming the intermediate ^{6}**3**. In ^{6}**TS$_{2/3}$** state (see in Fig.2), the Re gradually approaches to the methyl group. At the same time, the H2 escapes from C2 and moves to Re. Then Re inserts into the C2-H2 bond leading to the formation of the Re-H2 and Re-C2 bonds. Simultaneously the Re-C1 and Re-N connections are destroyed. In this step, the barrier is as high as 103 kJ/mol, while the exothermicity of the ^{6}**2**→^{6}**3** is only 12 kJ/mol. The next process is the fracture of C1-C2 bond. From the immediate ^{6}**3**, Re removes toward the N and H2 returns to the methylene, while the Re and C2 always keep the bonding. At the transition ^{6}**TS$_{3/4}$** point, the C1-C2 bond is gradually broken (C1···C2 is 1.93 Å) and N is attracted by Re forming a normal Re-N bonding (Re-N is 2.02 Å). In the mean time, the nitrilic NC bond is kept unchanged, see in Fig.2. The ^{6}**3**→^{6}**4** reaction turns over the transition state ^{3}**TS$_{3/4}$** with a high activation energy of 170 kJ/mol and is exothermic by about 48 kJ/mol.

Starting with the insertion complex ^{6}**4**, the agostic interaction occurs due to the C-H activation aroused by Re. In Fig.2, we can see the H3-migration from C2 to the Re forming the C-H insertion product ^{6}**5**. The complex ^{6}**5** relative to the reactants is endothermic by 20 kJ/mol and this process

should overcome the barrier by 154 kJ/mol. Next, the Re continues to activate the second C-H bond from the methylene. The H1 transfers from C2 to Re crossing the transition state ^{6}**TS$_{5/6}$** with a barrier of 164 kJ/mol to form CH≡Re(H)$_2$NC (^{6}**6**). However, the C-H bonding activation process need cross relatively higher transition barriers and are endothermic energies of 265 kJ/mol from ^{6}**4** to product ^{6}**6** which hardly occurred.

3.3 The Spin-Quartet Reaction Mechanism for Re (^{4}G) + CH$_3$CN system

The following reaction pathway is somewhat similar with the sextet state. The lowest quartet state is ^{4}G (d^5s^2) which lies 130 kJ/mol above the ground state with Baerends method. Different from the complex of Re···NCCH$_3$(^{6}**1**), Re is bonded with NC forming a linear structure in ^{4}ReNC-CH$_3$ (^{4}**1**), see in Fig.2. The first intermediate is formed releasing large energy by about 169 kJ/mol and the Re-N bond length is as short as 1.82 Å. However, the ^{4}**1** must convert over an obvious transition state ^{4}**TS$_{1/2}$** (about 70 kJ/mol) in order to proceed to the nitrile π complex η^2-Re(NC)CH$_3$ (^{4}**2**). Then, with the H migration from C2 to Re, Re approaching to C2 makes the skeleton structure Re-η^3- (N-C-C) (^{4}**3**) which would result in the breakage of C-C bond. Meanwhile the Re-C2 bond length becomes 2.06 Å, which is just the sum of the atomic radii of Re and C. This indicates that the Re-C single bond is formed. However, the bond length of Re-C1 from 1.98 Å (in ^{4}**2**) to 2.22 Å (in ^{4}**3**) makes the Re-C1 bond weaken. With the H drop to C2, both the C1-C2 and the Re-C1 split gradually. The IRC calculations have confirmed that transition state ^{4}**TS$_{2/3}$** and ^{4}**TS$_{3/4}$** are connected to intermediate ^{4}**3,** ^{4}**4** in the forward direction and to intermediate ^{4}**2,** ^{4}**3** in the backward direction, respectively. The activation energy values of transition barriers ^{4}**T$_{S2/3}$** and ^{4}**TS$_{3/4}$** are about 136 kJ/mol and 196 kJ/mol, respectively. So the latter is regarded as the rate-determining step. From intermediate ^{4}**4**, the reaction goes through a slight barrier (about 15 kJ/mol) to the CH$_2$=Re(H)NC (^{4}**5**). However, the excessive ^{4}**TS$_{5/6}$** (as high as about 155 kJ/mol) and product ^{4}**6** make this reaction step kinetically no advantage. The whole reaction process ends up to the product ^{4}**5** and is largely exothermic by about 275 kJ/mol.

3.4 The Spin-Doublet Reaction Mechanism for Re (^{2}D) + CH$_3$CN system

The doublet excited state ^{2}D (d^5s^2) lies 258 kJ/mol above the ground state Re. Similar with the quartet state, the ^{2}ReNC-CH$_3$ is formed immediately following a very large stabilization energy 272 kJ/mol relative to the reactant Re(^{2}D) + CH$_3$CN. After the high barriers of ^{2}**TS$_{2/3}$** (152 kJ/mol) and

^{2}**TS$_{3/4}$** (210 kJ/mol), the reaction arrives to the complex ^{2}**4**. However, the complex ^{2}**4** and ^{2}**5** would readily proceed to ^{2}**5** and ^{2}**6** because of the negligibly barriers of ^{2}**TS4/5** and ^{2}**TS5/6**. The energy of CH≡Re(H)$_2$NC (^{2}**6**) is much lower than that of the ^{4}**6** and ^{6}**6** and is the most stable product in the three spin states. The whole reaction on doublet pathway is hugely exothermic by about 468 kJ/mol.

3.5 Intersystem Crossing and the Conceivable Overall Reaction Pathway

The three reaction pathways of spin-restricted states above are merged in the Fig. 1 with the ground sextet spin state of Re (^{6}S) + CH_3CN as reference. The energies of reactants in ^{4}G and ^{2}D spin states lie 131 kJ/mol and 258 kJ/mol above that of ^{6}S. Then, the η^2-Re(NC)CH_3, η^3-HRe(NCCH_2), CH_3-ReNC, CH_2=Re(H)NC products all present quartet spin states as ground states in energy and are 77, 99, 104, 144 kJ/mol lower than that of the sextet ground reactant. And the final product CH≡Re(H)$_2$NC is doublet ground state and 210 kJ/mol lower than that of the sextet ground reactant. Here, the vibrational frequencies for the intermediates and product have also been analysed between experimental IR spectrum from Cho and Andrews[28] and the theoretical calculations (see in Table 3). Together with the energy and IR frequency, the ground intermediates and final products are determined.

Table 3. Theoretical and experimental vibrational frequencies (in cm^{-1}) of intermediates. Spin-state is indicated at left superscript of the frequencies.

Intermediates	Vibration model	B3LYP[a]	BPW91[a]	BP86	Exp[a]
Re···NCCH_3(**1**)	*ν*(CN-str.)	^{6}2363	^{6}2144	^{6}2111	2100
				^{4}1864	
				^{2}1805	
Re(NC)CH_3 (**2**)	*ν*(NRe-str.)	^{4}616	^{4}585	^{4}588	–
				^{6}474	
				^{2}650	
HRe(NCCH_2) (**3**)	*ν*(ReH-str.)			^{4}1943	–
				^{6}1865	
				^{2}2033	
CH_3-ReNC (**4**)	*ν*(NC-str.)	^{6}2081	^{6}1986	^{6}1965	2023
				^{4}1935	
				^{2}1932	
CH_2=Re(H)NC (**5**)	*ν*(ReH-str.)	^{4}2015	^{4}1981	^{4}1971	1921
				^{2}2138	

CH≡Re(H)$_2$NC (**6**)	ν(CN-str.)	^{2}2091	^{2}2015	^{6}1991 ^{2}2006 ^{4}1920 ^{6}1874	2028
	ν(ReH$_2$-twist) [d]	^{2}632	^{2}625	^{2}624	629
	ν(ReH$_2$-wag) [d]	^{2}604	^{2}591	^{2}594	607

a: from Ref.28 by Cho and Andrews.

On the first step, intermediate **1**, experimental spectra term (2100 cm^{-1} for CN stretching model) is more close to the calculation of the N-coordinate ^{6}Re···NCCH$_3$ (2111cm^{-1} for CN) rather than ^{4}ReNC-CH$_3$ (1864cm^{-1} for CN), although the energy value of ^{4}ReNC-CH$_3$ is relatively lower. From Fig.1, the structure in ^{6}Re···NCCH$_3$ with the undeformed NCCH$_3$ radical presents the formation very direct and easy. The mutable ^{6}Re···NCCH$_3$ immediately passes to a negligible transition state ^{6}**TS$_{1/2}$** to ^{6}**2**. So, this step is very fast from **1** to **2**.

Overall, the reaction could begin with the Re (^{6}S) + CH$_3$CN to the complex ^{6}Re···NCCH$_3$ (^{6}**1**) and proceed through a nearly nonexistent barrier ^{6}**TS$_{1/2}$**. Intersystem crossing may occur between ^{6}**TS$_{1/2}$** and ^{4}**2** near the Projected Crossing Point 1 **(PCP1)**. Also probably partially from the ^{4}ReNC-CH$_3$ via the ^{4}**TS$_{1/2}$** to the ^{4}**2**, however, relatively large barrier and unmatched frequency verification (^{4}**2**) make it being the secondary probability. Then on the quartet reaction pathway, reaction continues to turn over the two hills of ^{4}**TS$_{2/3}$** and ^{4}**TS$_{3/4}$** to the ^{4}**3** and to ^{4}**4**. A slight slope ^{4}**TS$_{4/5}$** makes the product ^{4}**5** emerge easily. Lastly, there may be the intersystem crossing near the **PCP2** from ^{4}**5** to the insignificant transition ^{2}**TS$_{5/6}$**, the reaction finally comes to the ground product ^{2}**6** which is in the doublet state. If the excited state ^{2}Re atom is formed, the process also partially directly goes from the ^{2}**2** via ^{2}**TS$_{2/3}$** and ^{2}**TS$_{3/4}$** to ^{2}**3** and ^{2}**4**, then via the tiny barrier ^{2}**TS$_{4/5}$** and ^{2}**TS$_{5/6}$** to the ^{2}**5** and ^{2}**6**. The adjacent energy of different spin states makes also other probability for the possible reaction pathways. However, spin-flip processes could be more likely to occur between two similar geometries, larger difference in geometries makes it more barriers between the two spin states. Therefore, the reaction may arrive at the intermediate ^{4}**2**, ^{4}**3**, ^{4}**4**, ^{4}**5** then pass through the spin crossing to ^{2}**6**. A possible low-energy pathway from sextet to doublet state is:

$$\text{Re } (^6\text{S}) + \text{CH}_3\text{CN} \rightarrow \eta^1\text{-ReNCCH}_3\ (^6\mathbf{1}) \rightarrow {}^6\mathbf{TS_{1/2}} \rightarrow \mathbf{PCP1} \rightarrow \eta^2\text{-Re(NC)CH}_3\ (^4\mathbf{2})$$
$$\rightarrow {}^4\mathbf{TS_{2/3}} \rightarrow \eta^3\text{-HRe(NCCH}_2)\ (^4\mathbf{3}) \rightarrow {}^4\mathbf{TS_{3/4}} \rightarrow \text{CH}_3\text{-ReNC}\ (^4\mathbf{4}) \qquad (2)$$

$\rightarrow {}^{4}\mathbf{TS_{4/5}} \rightarrow CH_2{=}Re(H)NC\ ({}^{4}\mathbf{5}) \rightarrow \mathbf{PCP2} \rightarrow {}^{2}\mathbf{TS_{5/6}} \rightarrow CH{\equiv}Re(H)_2NC\ ({}^{2}\mathbf{6})$

The whole reaction would be exothermic from the ground reactants to the product $^{2}\mathbf{6}$ by 210 kJ/mol. The spin contamination problem is often occurred in unrestricted calculations due to UHF wave function is not the eigenfunction of the spin operator $\hat{\mathbf{S}}^2$. But this is not happened in DFT investigations at ZORA-BP86-TZ2P/STO level in Re + CH_3CN system. Compare with the calculated and expectation values of $<S^2>$, the small deviations could be ignored. Due to the basis sets used shortage and the B3LYP deficiency, Cho and Andrews provided higher calculation values[28] which differ with ours. For the first intermediate $^{6}\mathbf{1}$, their theoretical frequency of BPW91 was in good agreement with the observed values (see Table 3), but the B3LYP even couldn't reproduce the reasonable geometry of the complex $^{6}\mathbf{1}$. So, the whole reaction pathway using the B3LYP method may have an uncertainty with critical defects.

3.6 Minimum Energy Crossing Points (MECP) for the multi-spin states

Density functional theory (DFT) uses electron density as variable for multi-electron system, non-degenerate ground state corresponds to the ground electron density, that is also the unique functional. In general, DFT as a wonderful model could optimize the equilibrium configurations by a single determinant wavefunction for most chemical systems. Among these, "Aufbau principle" always be fulfilled in the electronic configuration, that means the highest occupied molecular orbitals lowest in energy than all unoccupied orbitals at DFT ground state which proved by Janak[63]. However, when two adiabatic states in near-degenerate, two near-energy orbitals often make the empty orbital below the occupied orbital. Therefore, the single-determinant DFT method couldn't correctly describe the adiabatic states. In these cases, nondynamical correlation effects become crucial such as at the intersystem crossing point.

Traditional method to such for MECP would adopt multiple-configuration wave functional ones like CASSCF or MCSCF[32-38] for rational orientation in transition region. Here, we have proposed one simple DFT Fractional Orbital Occupation Number (FON) approach based procedure[39] to simulate the non-dynamical correlation effects for searching for the MECP in the LECR.

To better analyze the change of electron configurations for spin-flip process, at the PCP1 and PCP2 two points, a six frontier MOs of pure-spin states ($^{6}\mathbf{TS_{1/2}}$ and $^{4}\mathbf{TS_{1/2}}$, $^{4}\mathbf{5}$ and $^{2}\mathbf{5}$) energy level

diagram both α and β are listed in Fig.3. There are six α and one β spin electrons and five α and two β spin electrons occupying the frontier MOs in ^{6}**TS$_{1/2}$** and ^{4}**TS$_{1/2}$**, respectively. If the reaction process wants to jump from sestet PES to quartet state at the first PCP, it needs one α electron transfer to β-spin state. The highest occupied molecular orbital (HOMO) is the 25A (α) and the lowest unoccupied molecular orbital (LUMO) is 21A (β) in ^{6}**TS$_{1/2}$**. Meanwhile, in ^{4}**TS$_{1/2}$**, the HOMO is 21A (β), and the LUMO is 25A (α). So, near the transition state **TS$_{1/2}$**, say as at the Projected Crossing Point 1, the spin-flip process could be occurred. PCP2 is located near the ^{2}**5** and ^{4}**5** where the intersystem crossing could occur between quartet- and doublet-spin PESs similar to PCP1 (See ^{4}**5** and ^{2}**5** in Fig.3). One electron flips from 24A (α) to 22A (β) orbital.

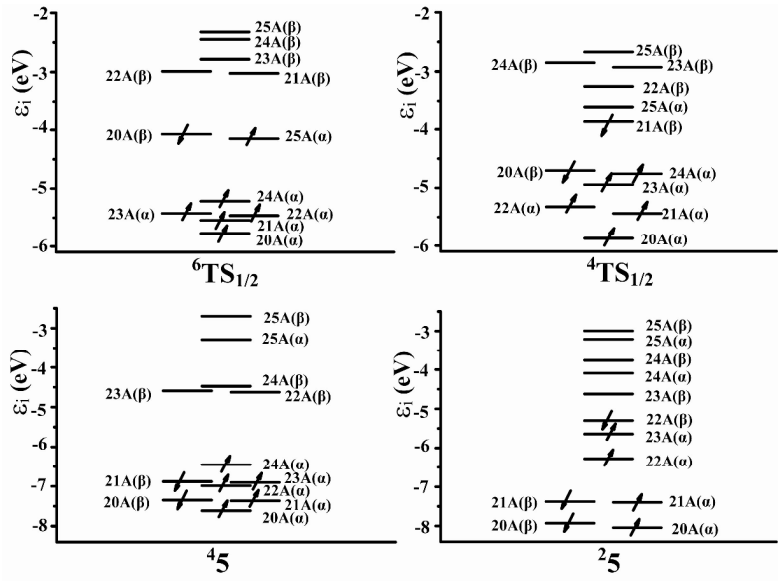

Fig. 3 The energy level diagram for frontier spin orbitals with the 7 HOMOs and 5 LUMOs in ^{6}**TS$_{1/2}$** and ^{4}**TS$_{1/2}$,** ^{4}**5** and ^{2}**5**, respectively (ε in eV).

To search for the MECP, we start from the so-called projected crossing point 1 (PCP1) in which the sextet and quartet states have same energy at the same projected reaction coordinate (in a two dimensional diagram they seem crossing each other) but with different other geometric parameters in a 3N-7 dimension (N=9-atomic system). As shown in Fig.4.a), when the angle $\angle_{\mathbf{Re\text{-}N\text{-}C1}}$ equals to 85.57°, $E(^{6}A)_{\mathbf{PCP1}} = E(^{4}A)_{\mathbf{PCP1}}$. Anyhow, the Frank-Condon principle is not satisfied due to the different geometries of the two spin states. Next, use the FON-DFT procedure to determine the geometric structures for MECP. In order to fulfil the "Aufbau principle", the occupation number n of $25A(\alpha)^{n}$ and $21A(\beta)^{1-n}$ is optimized and all of the geometry parameters are optimized simultaneity

except for the reaction coordinate $\angle_{\mathbf{Re\text{-}N\text{-}C1}}$ kept as the constant value 85.57°. Along with the fractional occupation number n changing, the orbital energy of $25A(\alpha)^n$ drops and $21A(\beta)^{1-n}$ rises up (see in Fig.4b and 4d). At the point of n=0.450, the two energy curves intersect and the transition geometry is close to the MECP1. Then we need to verify whether this transition structure satisfies the Franck-Condon principle, i.e. $E(^6A)_{\mathbf{MECP1}} = E(^4A)_{\mathbf{MECP1}}$ at the same point. If not, once more searching process is needed. However, that is infrequent. With the transition structure, there is only 0.9 kJ/mol energy difference between sextet and quartet spin states, which is within in our convergent limitation. At the MECP1, reaction pathway transits from the sextet spin state to quartet spin state.

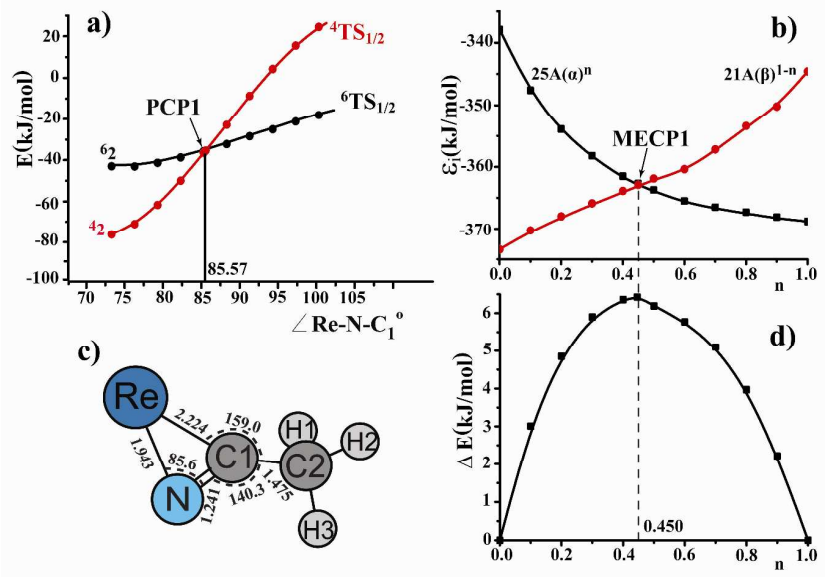

Fig. 4 a): The optimized energy surface E along the reaction coordinate $\angle_{\mathbf{Re\text{-}N\text{-}C1}}$ between the transition state $\mathbf{TS_{1/2}}$ to Re(NC)CH_3 (**2**) in the pure sextet and quartet spin states, respectively; b) and d) : Under the DFT-FON procedure, the $25A(\alpha)^n$ and $21A(\beta)^{1-n}$ orbital energy curves versus FON *n* for mixed ensemble $n(^6A) + (1\text{-}n)(^4A)$ and the ensemble FON energy *E*; c): Structural parameters of the MECP1. (E and ε_i in kJ/mol, bond lengths in Å, bond angles in degrees).

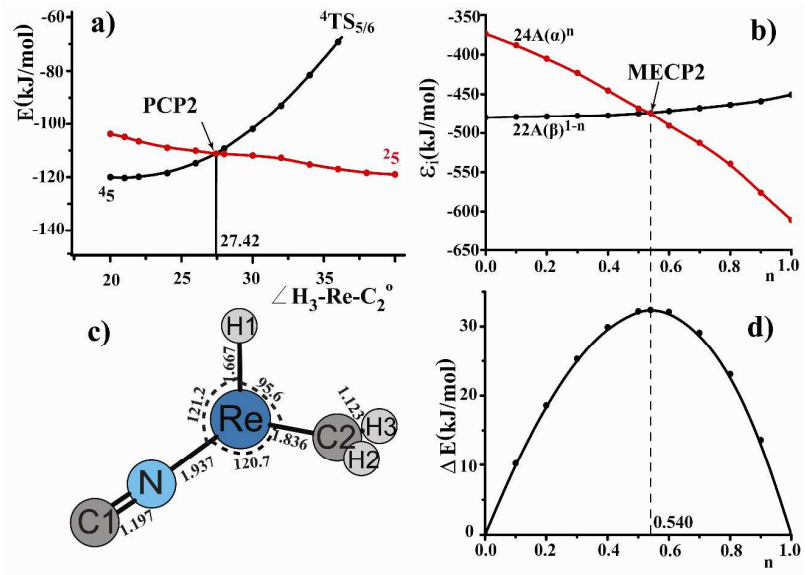

Fig. 5 a): The optimized energy surface E along the reaction coordinate $\angle_{H3\text{-}Re\text{-}C2}$ between the CH_2=Re(H)NC (**5**) to $\mathbf{TS_{5/6}}$ in the pure quartet and doublet spin states, respectively; b) and d) : Under the DFT-FON procedure, the $24A(\alpha)^n$ and $22A(\beta)^{1-n}$ orbital energy curves versus FON n for mixed ensemble $n(^4A) + (1\text{-}n)(^2A)$ and the ensemble FON energy E; c): Structural parameters of the MECP2. (E and ε_i in kJ/mol, bond lengths in Å, bond angles in degrees).

Similarly, PCP2 appears at $\angle_{H3\text{-}Re\text{-}C2}$ = 27.42° along the reaction pathway from $^4\mathbf{5}$ to $^2\mathbf{TS_{5/6}}$. When n = 0.540, the MO $25A(\alpha)^n$ is equal to $22A(\beta)^{1-n}$. The optimized transition structure displays at the left bottom of Fig.5. Based on this geometric structure, there is only 0.5 kJ/mol energy difference between quartet and doublet spin states. $E(^4A)_{\mathbf{MECP2}} = E(^2A)_{\mathbf{MECP2}}$ i.e. the Franck-Condon principle could come into existence. Meanwhile, the electronic configurations of both MECP1 and MECP2 under different spin-symmetry also obey the "aufbau principle"[63].

3.6 Molecular Structure and Bonding

The complexes **4, 5** were found in the reaction of Re atom with acetonitrile as the major intermediates and the quartet spin states are assumed the most generated ones than the sextet and doublet states. However, the doublet spin state of complex **6** was determined as the final product. To understand more clearly the variance, it is necessary to make more detailed analysis on the molecular structure for **5** and **6** with three spin states.

The equilibrium geometries and energies of CH_2=Re(H)NC (**5**) and CH≡$Re(H)_2$NC (**6**) in three spin states are displayed in Fig.2 and Table 2. Here are the Natural Bonding Orbital (NBO) and harmonic vibrational frequencies analysis in Table 4. The present BP86 reproduced all vibrational frequencies of complex ^{4}**5** and ^{2}**6** which are in agreement well with the experimental IR values. For example, the ν (C1-N) observable IR spectrum is 2028 cm^{-1} in the final products which is very closed with the theoretical ^{2}**6** value 2006 cm^{-1}, far from the ^{4}**6** and ^{6}**6** values 1920 cm^{-1} and 1874 cm^{-1}. And the *ν*(Re-H) in-plane bend of ^{2}**5,** ^{4}**5** and ^{6}**5** are 700 cm^{-1}, 615 cm^{-1}, 581 cm^{-1} in DFT frequencies, only the ^{4}**5** value is nearest the IR one (639 cm^{-1}). These results also fit the computed ones with BPW91 from Cho and Andrews[28].

The bond length of Re-C2 for ^{6}**5** geometry is 2.07Å; however, the values for ^{4}**5** and ^{2}**5** shorten to 1.86 Å and 1.78 Å, respectively (see in Fig.2). The shorter Re-C2 bond length is, the stronger the bonding energy would be. The energy value for ^{6}**5** is far higher than that of the quartet and doublet states by about 125 kJ/mol. From the NBO analysis, the Wiber Bonding Order (WBO) of Re-C2 for ^{4}**5** (1.78) and ^{2}**5** (2.15) are greater than that of ^{6}**5** (0.85). H1 atom in ^{2}**5** shows forceful departure from C2 to Re, that makes the H3 and H1 shaping in the same side of Re-C2, the ^{2}**5** geometry emerges evident active. The energy pathway also goes through a fully unhindered transition $\mathbf{TS_{5/6}}$ after the ^{2}**5** suggestively. However, the complex ^{4}**5** has a Cs symmetric structure and is relatively stable. From the NBO analysis, the Weinhold charges of Re and C2 are 0.87 (Re in ^{4}**5**), 0.37(Re in ^{2}**5**) and -0.61(C2 in ^{4}**5**), -0.32(C2 in ^{2}**5**) in quartet and doublet spin states, respectively, which indicates the Re-C2 bond with more polarized property in quartet state.

The Weinhold charges haven't much different for the three spin states in CH≡$Re(H)_2$NC (**6**). However, the Re-C2 bond distance in doublet state (1.72 Å) is shorter than in other two spin states (1.84 Å, 2.04 Å). The Wiberg Bond Orders for Re-C2 are 2.65 (^{2}**6**), 1.32 (^{4}**6**) and 0.95 (^{6}**6**), which shows the most stable structure in doublet state. The final products **6** have the similar geometric structures in the three different spin states. The compounds with higher spin multiplicity usually are more unstable than with the lower ones.

Table 4. NBO, WBO and Frequency (ν) Data of the Major Products CH_2=Re(H)NC (**5**) and CH≡$Re(H)_2$NC (**6**) in the three Spin States.

Property	CH_2=Re(H)NC			CH≡$Re(H)_2$NC		
	^{2}**5**	^{4}**5**	^{6}**5**	^{2}**6**	^{4}**6**	^{6}**6**
C2 [a]	$2s^{1.23}2p^{3.07}$	$2s^{1.24}2p^{3.36}$	$2s^{1.34}2p^{3.26}$	$2s^{1.24}2p^{2.84}$	$2s^{1.37}2p^{2.76}$	$2s^{1.45}2p^{2.78}$
Re [a]	$5d^{5.78}6s^{0.71}$	$5d^{5.33}6s^{0.61}$	$5d^{5.24}6s^{0.66}$	$5d^{5.81}6s^{0.62}$	$5d^{5.65}6s^{0.63}$	$5d^{5.51}6s^{0.64}$
ρ_α(Re) [b]	1.14	3.14	3.93	1.17	2.03	2.94
ρ_α(C2) [b]	-0.12	-0.22	0.92	-0.13	0.78	1.84
ρ_α(H1) [b]	-0.05	-0.07	-0.04	-0.05	-0.06	-0.02
q(C2) [c]	-0.32	-0.61	-0.62	-0.10	-0.15	-0.25
q(CH_2/CH) [c]	CH_2:0.07	CH_2:-0.17	CH_2:-0.25	CH:0.10	CH:0.02	CH:-0.12
q(C1) [c]	0.29	0.27	0.26	0.30	0.30	0.27
q(N) [c]	-0.77	-0.84	-0.80	-0.81	-0.75	-0.71
q(CN) [c]	-0.48	-0.57	-0.54	-0.51	-0.45	-0.44
q(Re) [c]	0.37	0.87	0.83	0.31	0.36	0.47
v(ReH str)[d]	2138	1971(1921)	1991			
v(Re-H ip bend) [d]	700	615(639)	581			
v(ReH_2-twist) [d]				624(629)[f]	814	657
v(ReH_2-wag) [d]				594(607)	738	564
v(ReH_2-asym str)[d]				2092(2032)	1942	2066
v(ReH_2-sym str)[d]				2118(2088)	2102	2074
v (C1-N)[d]	1972	1971	1923	2006(2028)	1920	1874
WBO_{Re-C2} [e]	2.15	1.78	0.85	2.65	1.32	0.95
WBO_{Re-N} [e]	0.75	0.64	0.72	0.65	0.75	0.85
WBO_{Re-H3} [e]	0.91	0.80	0.85	0.84	0.66	0.83

[a] Weinhold electron configuration, [b] atomic α-spin density, [c] Weinhold charge, [d] Frequency in cm^{-1} at ZORA-BP86-TZ2P/STO DFT level, [e] Wiberg bond order, [f] Experimental IR frequencies in parentheses from Ref. [28].

4. Conclusions

In this paper, we have made detailed investigation on the reaction of Re atom with acetonitrile theoretically. Three adiabatic spin states (sextet, quartet and doublet) PESs have been studied to explore the whole reaction process at the relativistic DFT level. Here are some conclusions as follows：

1) There are six stationary states (**1** to **6**) and five transition states (**$TS_{1/2}$** to **$TS_{5/6}$**), among them, the underlined were identified by Cho and Andrews experimentally. The whole minimum energy reaction pathway could be realized through sextet-reactants to doublet-products as follows:

^{6}Re+CH_3CN → η^1-$ReNCCH_3$ (^{6}**1**) → ^{6}**$TS_{1/2}$** → **MECP1**→

$$\eta^2\text{-Re(NC)CH}_3\ (^4\mathbf{2}) \rightarrow {}^4\mathbf{TS_{2/3}} \rightarrow \eta^3\text{-HRe(NCCH}_2)\ (^4\mathbf{3}) \rightarrow {}^4\mathbf{TS_{3/4}} \rightarrow \quad (3)$$

$$\underline{\text{CH}_3}\text{-}\underline{\text{ReNC}}\ (^4\mathbf{4}) \rightarrow {}^4\mathbf{TS_{4/5}} \rightarrow \underline{\text{CH}_2}\text{=Re(H)}\underline{\text{NC}}\ (^4\mathbf{5})$$

$$\rightarrow \mathbf{MECP2} \rightarrow {}^2\mathbf{TS_{5/6}} \rightarrow \text{CH}\equiv\text{Re(H)}_2\underline{\text{NC}}\ (^2\mathbf{6})$$

Starting from the ground reactants ^{6}Re with CH_3CN, one η^1-σ-interaction between Re atom and N atom in CH_3CN directly makes the formation of the intermediate ^{6}**1**. However, the ^{6}**1** is very reactive, Re moves rapidly to the top center of CN group forming the η^2-π-complex ^{4}**2** through an ignorable barrier. Skewing right along the top of NCC radical, one η^3-π-interaction makes Re interact with the CH_2 group forming the $HRe(NCCH_2)$ (^{4}**3**) which would contribute to break the C-C bonding. From CH_3-ReNC (^{4}**4**) with the structural rearrangement, the reaction goes on with two H successive migration from C to Re and finally generates the product ^{2}**6**.

2) This process includes three spin states and two spin inversion. Between $\mathbf{TS_{1/2}}$ and **2**, the sextet and quartet pure-spin reaction pathway have been crossed and there should be one LECR. The DFT-FON procedure is applied to determine the MECP1 and makes the intermediate ^{4}**2** by about 30 kJ/mol energy lower than the high-sextet one ^{6}**2**. The second spin crossing point was located near the product **5** on the quartet and doublet states. Through the spin inversion, reaction avoids the large transition barrier of $^4\mathbf{TS_{5/6}}$ (higher by 157 kJ/mol than $^2\mathbf{TS_{5/6}}$) and goes through the negligible barrier of $^2\mathbf{TS_{5/6}}$ to the final product $CH\equiv Re(H)_2NC$ (^{2}**6**). Both MECPs are verified corresponding to the Frank-Condon principle and "aufbau principle". The overall reaction starts from the sextet PES and passes through the MECP1 into the quartet PES, then finally through MECP2 ends in the product ^{2}**6**. The whole process could be exothermic by 210 kJ/mol.

3) The high-spin complex ^{6}**1** is regarded as the intermediate **1** though the energy of quartet-spin complex ^{4}**1** is little lower than the ^{6}**1**. The frequency analysis between experimental and theoretical confirmed the existence of high-spin complex ^{6}**1** (deviated less than 11 cm^{-1}) but not the big difference (about 236 cm^{-1}) for ^{4}**1**. The structure for the undeformed $NCCH_3$ group in ^{6}Re···$NCCH_3$ presents the formation very direct and easy. The large difference between the insignificant barrier of $^6\mathbf{TS_{1/2}}$ and large barrier of $^4\mathbf{TS_{1/2}}$ also makes the ^{6}Re···$NCCH_3$ to $^6\mathbf{TS_{1/2}}$ unimpeded. All intermediates and products for the three spin states are also investigated by frequency analysis, and the other minimum structures are all in accordance with the experimental IR spectrum.

4) The products CH_2=Re(H)NC and CH≡$Re(H)_2$NC in three spin states are analyzed in detail. CH≡$Re(H)_2$NC have the low-spin doublet state while CH_2=Re(H)NC is in quartet state.

Acknowledgement. We acknowledge financial support by the National Nature Science Foundation of China (No. 20773086).

Notes and references

1. P. B. Armentrout and J. L. Beauchamp, *Acc. Chem. Res.,* 1989, **22**, 315.

2. P. B. Armentrout, *Rev. Phys. Chem*, 1990, **41**, 313.

3. P. B. Armentrout, *Science*, 1991, **251**, 175.

4. D. Schröder, S. Shaik and H. Schwarz, *Acc. Chem. Res.*, 2000, **33**, 139.

5. S. Shaik, D. Danorich, A. Fiedler, D. Schröder and H. Schwarz, *Helv.Chim.Acta*., 1995, **78**, 1393.

6. D. Danorich and S. Shaik, *J.Am.Chem.Soc.,* 1997, **119**,1773.

7. R. Poli and J. N. Harvey, *Chem. Soc. Rev*., 2003, **32**, 1.

8. J. N. Harvey, *Phys. Chem. Chem. Phys*., 2007, **9**, 331.

9. P. Gütlich, Y. Garcia and T. Woike, *Coord. Chem. Rev.*, 2001, **219**, 839.

10. P. Gütlich, Y. Garcia and H. A. Goodwin, *Chem. Soc. Rev.*, 2000, **29**, 419.

11. K. Eller and H. Schwarz, *Chem. Rev.*, 1991, **91**, 1121.

12. K. Eller, *Coord. Chem. Rev.*, 1993, **126**, 93.

13. J. C. Weisshaar, *Acc.Chem.Res.*, 1993, **26**,213.

14. S.Afzaal and B. S.Freiser, *Chem. Phys. Lett.,* 1994, **218**, 254.

15. D. A. Plattner, *Topics Curr. Chem.*, 2003, **225**, 153.

16. L. Operti and R. Rabezzana, *Mass Spectrom. Rev.*, 2006, **25**, 483.

17. J. Roithova and D. Schröder, *Chem. Rev.*, 2010, **110**, 1170.

18. H. G. Cho and L. Andrews, *Dalton Trans.*, 2011, **40**, 11115.

19. H. G. Cho and L.Andrews, *Dalton Trans.*, 2009, **30**, 5858.

20. H. G. Cho, L.Andrews, B.Vlaisavljevich and L.Gagliardi, *Organometallics*, 2009, **28**, 5623.

21. H. G. Cho, J. T. Lyon and L. Andrews, *J. Phys. Chem. A*, 2008, **112**, 6902.

21. H. G. Cho and L.Andrews, *J. Am. Chem. Soc.,* 2008, **130**, 15836.

23. H. G. Cho and L.Andrews, *Organometallics*, 2008, **27**, 1786

24. H. G. Cho and L.Andrews, *J. Phys. Chem. A,* 2005, **109**, 6796.

25. H. G. Cho and L.Andrews, *J. Phys. Chem. A,* 2010, **114**, 5997.

26. H. G. Cho and L.Andrews, *J. Phys. Chem. A,* 2010, **114**, 891.

27. H. G. Cho and L.Andrews, *J.Organomet.Chem.,* 2012, **703**, 25

28. H. G. Cho and L.Andrews, *Organometallics*, 2012, **31**, 6095

29. R. Poli, *J. Organomet. Chem.,* 2004, **689**, 4291.

30. F. Neese, T. Petrenko, D. Ganyushin and G. Olbrich, *Coord Chem Rev.*, 2007, **251**, 288.

31. D.G. Fedorov, S. Koseki, W. Michael and M.S. Gordon, *Int Rev Phys Chem.*, 2003, **22**, 551.

32. D. R. Yarkony, *J. Phys. Chem.*, 1993, **97**, 4407.

33. T. Chachiyo and J. H. Rodriguez, *J. Chem. Phys.,* 2005, **123**, 094711.

34. Z. Guo, Z. Ke, D. L. Phillips and C. Zhao, *Organometallics,* 2007, **27**, 181.

35. N. Koga, K. Morokuma, *Chem. Phys. Lett.,* 1985, **119**, 371.

36. J. Schoeneboom and W. Thiel, *J. Am. Chem. Soc.*, 2004, **126**, 4017.

37. J. N. Harvey, M. Aschi, H. Schwarz and W. Koch, *Theor. Chim. Acta.*, 1998, **99**, 95.

38. E. L. Øiestad, J. N. Harvey and E. Uggerud, *J. Phys. Chem. A.*, 2000, **104**, 8382.

39. (a). S. G. Wang and W. H. E. Schwarz, *J. Chem. Phys.,* 1996, **105**, 4641. (b). S. G. Wang, X. Y. Chen and W. H. E. Schwarz, *J. Chem. Phys.,* 2007, **126**, 124109. (c). H. Chermette, I. Ciofini, F. Mariotti and C. Daul, *J. Chem. Phys.,* 2001, **115**, 11068. (d). H. Chermette, I. Ciofini, F. Mariotti and C. Daul, *J. Chem. Phys.,* 2001, **114**, 1447.

40. J. Li, X. Y. Chen, Y. X. Qiu and S. G. Wang, *J. Phys. Chem. A,* 2009, **113**, 8471.

41. (a). Q. Li, Y. X. Qiu, X. Y. Chen, W.H.E. Schwarz and S.G. Wang, *Phys. Chem. Chem. Phys.*, 2012, **14**, 6833. (b). Q. Li, X. Y. Chen, Y. X. Qiu, and S.G. Wang, *J. Phys. Chem. A.*, 2012, **116**, 5019.

42. Y. Xiao, X. Y. Chen, Y. X. Qiu and S. G. Wang, *J.Mol. Model.*, 2013, **9**, 4003.

43. E. J. Baerends, D. E. Ellis and P. Ros, *Chem. Phys.*, 1973, **2**, 41.

44. T. Ziegler, A. Rauk and E. J. Baerends, *Theor. Chim. Acta.*, 1977, **43**, 261

45. G. te Velde and E. J.Baerends, *J. Comput. Phys.*, 1992, **99**, 84.

46. A. Rosén and I. Lindgren, *Phys. Rev.*, 1968, **176**, 114.

47. E. van Lenthe and E. J. Baerends, *J. Comput. Chem.*, 2003, **24**, 1142.

48. S. H. Vosko, L. W. and M.Nusair, *Can. J. Phys.,* 1980, **58**, 1200.

49. A. D. Becke, *Phys. Rev. A*, 1988, **38**, 3098.

50. J. P. Perdew, *Phys. Rev. B*, 1986, **33**, 8822.

51. J. P. Perdew, J.A. Chevary, S. H. Vosko, K. A.Jackson, M. R. Pederson, D. J.Singh and C. Fiolhais, *Phys. Rev. B,* 1992, **46**, 6671.

52. J. P. Perdew, K. Burke and M. Ernzehof, *Phys. Rev. Lett.*, 1996, **77**, 3865.

53. E. van Lenthe, E. J.Baerends and J. G. Snijders, *J. Chem. Phys.,* 1994, **101**, 9783.

54. L. Deng and T. Ziegler, L. Fan, *J. Chem. Phys.,* 1993, **99**, 3823.

55. L. Deng and T. Ziegler, *Int. J. Quantum Chem.,* 1994, **52**, 731.

56. K. A. Wiberg, *Tetrahedron*, 1968, **24***,* 1083.

57. A. E. Reed, L. A. Curtiss and F. Weinhold, *Chem. Rev.,* 1988, **88**, 899.

58. M. J. Frisch, G. W. Trucks, H. B. Schlegel, G. E. Scuseria, M. A. Robb, J. R. Cheeseman, G. Scalmani, V. Barone, B. Mennucci, G. A. Petersson, H. Nakatsuji, M. Caricato, X. Li, H. P. Hratchian, A.F. Izmaylov, J. Bloino, G. Zheng, J. L. Sonnenberg, M. Hada, M. Ehara, K. Toyota, R. Fukuda, J. Hasegawa, M. Ishida, T. Nakajima, Y. Honda, O. Kitao, H. Nakai, T. Vreven, J. A. Montgomery, Jr.. J. E. Peralta, F. Ogliaro, M. Bearpark, J. J. Heyd, E. Brothers, K. N. Kudin,V. N. Staroverov, R. Kobayashi, J. Normand, K. Raghavachari, A. Rendell, J. C. Burant, S. S. Iyengar, J. Tomasi, M. Cossi, N. Rega, J. M. Millam, M. Klene, J. E. Knox, J. B. Cross, V. Bakken, C. Adamo, J. Jaramillo, R. Gomperts, R. E. Stratmann, O. Yazyev, A. J. Austin, R. Cammi, C. Pomelli, J. W. Ochterski, R. L.Martin, K. Morokuma, V. G. Zakrzewski, G. A. Voth, P. Salvador, J. J. Dannenberg, S. Dapprich, A. D. Daniels, O. Farkas, J. B. Foresman, J. V. Ortiz, J. Cioslowski and D. J. Fox, Gaussian 09, Revision A.02, Gaussian, Inc., Wallingford, CT, 2009.

59. D.Andrae, U. Häußermann, M. Dolg, H. Stoll and H. Preuß, *Theor. Chim. Acta.,* 1990, **77**, 123.

60. K. Raghavachari and G. W. Trucks, *J. Chem. Phys.,* 1989, **91**, 1062.

61. NIST Chemistry Webbook, NIST Standard Reference Data Base Number 69, http://physics.nist.gov/PhysRefDate/Handbook/Tables/rheniumtable5.htm.

62. E. J. Baerends, V. Branchadell and M. Sodupe, *Chem. Phys. Lett.*, 1997, **265**, 481.

63. J. F. Janak, *Phys. Rev. B* 1978, **18**, 7165.

Investigation on Spin-Flip Reaction of Re + CH_3CN by Relativistic Density Functional Theory

Yi Xiao, Wen-Xin Ji, Wei-Xu, Xian-Yang Chen, and Shu-Guang Wang*

The minimal energy reaction pathway of Re+CH3CN has been investigated. The minimal energy crossing point is determined with the help of DFT fractional occupation-number (FON) approach.